

through Wilczek production [10] of an on-shell scalar state A^0 : $\Upsilon(1S) \rightarrow \gamma A^0$, $A^0 \rightarrow$ invisible. Such low-mass Higgs states appear in several extensions of the Standard Model [11]. Constraining the low-mass Higgs sector is important for understanding the Higgs discovery reach of high-energy colliders [12]. The BF for $\Upsilon(1S) \rightarrow \gamma A^0$ is predicted to be as large as 5×10^{-4} , depending on m_{A^0} and couplings [13]. If there is also a low-mass neutralino with mass $m_\chi < m_{A^0}/2$, the decays of A^0 would be predominantly invisible [14].

For multibody $\Upsilon(1S) \rightarrow \gamma\chi\bar{\chi}$ decays, the current 90% confidence level (C.L.) BF upper limit, based on a data sample of $\sim 10^6$ $\Upsilon(1S)$ decays, is of order 10^{-3} [15]. The limit on two-body $\Upsilon(1S) \rightarrow \gamma + X$, $X \rightarrow$ invisible decays is $\mathcal{B}(\Upsilon(1S) \rightarrow \gamma + X) < 3 \times 10^{-5}$ for $m_X < 7.2$ GeV [3]. The limit on invisible decays of $\Upsilon(1S)$ is $\mathcal{B}(\Upsilon(1S) \rightarrow \chi\bar{\chi}) < 3.0 \times 10^{-4}$ [7].

This Letter describes a high-statistics, low-background search for decays $\Upsilon(1S) \rightarrow \gamma +$ invisible, characterized by a single energetic photon and a large amount of missing energy and momentum. This is the first search of this kind to use the $\Upsilon(1S)$ mesons produced in dipion $\Upsilon(2S) \rightarrow \pi^+\pi^-\Upsilon(1S)$ transitions. We search for both resonant two-body decays $\Upsilon(1S) \rightarrow \gamma A^0$, $A^0 \rightarrow$ invisible, and nonresonant three-body processes $\Upsilon(1S) \rightarrow \gamma\chi\bar{\chi}$. For the resonant process, we assume that the decay width of the A^0 resonance is negligible compared to the experimental resolution [16]. We further assume that both the A^0 and χ particles have zero spin. The decays $\Upsilon(1S) \rightarrow \gamma\chi\bar{\chi}$ are modeled with phase-space energy and angular distributions, which corresponds to S-wave coupling between the $b\bar{b}$ and $\chi\bar{\chi}$.

The analysis is based on a sample corresponding to an integrated luminosity of 14.4 fb^{-1} collected on the $\Upsilon(2S)$ resonance with the *BABAR* detector at the PEP-II asymmetric-energy e^+e^- collider at the SLAC National Accelerator Laboratory. This sample corresponds to $(98.3 \pm 0.9) \times 10^6$ $\Upsilon(2S)$ decays. We also employ a sample of 28 fb^{-1} accumulated on the $\Upsilon(3S)$ resonance ($\Upsilon(3S)$ sample) for studies of the continuum backgrounds. Both $\Upsilon(3S) \rightarrow \pi^+\pi^-\Upsilon(2S)$ and $\Upsilon(3S) \rightarrow \pi^+\pi^-\Upsilon(1S)$ decays produce a dipion system that is kinematically distinct from the $\Upsilon(2S) \rightarrow \pi^+\pi^-\Upsilon(1S)$ transition. Hence, the $\Upsilon(3S)$ events passing our selection form a pure high-statistics continuum QED sample. For selection optimization, we also use 1.4 fb^{-1} and 2.4 fb^{-1} datasets collected about 30 MeV below the $\Upsilon(2S)$ and $\Upsilon(3S)$ resonances, respectively (off-peak samples). The *BABAR* detector, including the tracking and particle identification systems, the electromagnetic calorimeter (EMC), and the Instrumented Flux Return (IFR), is described in detail elsewhere [17, 18].

Detection of low-multiplicity events requires dedicated trigger and filter lines. First, the hardware-based Level-1 (L1) trigger accepts single-photon events if they contain at least one EMC cluster with energy above 800 MeV. A

collection of L1 trigger patterns based on drift chamber information selects a pair of low-momentum pions. Second, a software-based Level-3 (L3) trigger accepts events with a single EMC cluster with the center-of-mass (CM) energy $E_\gamma^* > 1$ GeV [19], if there is no charged track with transverse momentum $p_T > 0.25$ GeV originating from the e^+e^- interaction region. Complementary to this, a track-based L3 trigger accepts events that have at least one track with $p_T > 0.2$ GeV. Third, an off-line filter accepts events that have exactly one photon with energy $E_\gamma^* > 1$ GeV, and no tracks with momentum $p^* > 0.5$ GeV. A nearly independent filter accepts events with two tracks of opposite charge, which form a dipion candidate with recoil mass (defined below) between 9.35 and 9.60 GeV.

The analysis in the low-mass region $m_{A^0} \leq 8$ GeV ($m_\chi \leq 4$ GeV), which corresponds to photon energies $E_\gamma^* > 1.1$ GeV, requires the single-photon or the dipion trigger/filter selection to be satisfied; the trigger/filter efficiency for signal is 83%. In the high-mass region, $7.5 \leq m_{A^0} \leq 9.2$ GeV ($3.5 \leq m_\chi \leq 4.5$ GeV), we only accept events selected with the dipion trigger/filter, since a significant fraction of this region lies below the energy threshold for the single-photon selection. This selection has an efficiency of 12.5% for signal events.

We select events with exactly two oppositely-charged tracks and a single energetic photon with $E_\gamma^* \geq 0.15$ GeV in the central part of the EMC ($-0.73 < \cos \theta_\gamma^* < 0.68$). Additional photons with $E_\gamma^* \leq 0.12$ GeV can be present so long as their summed laboratory energy is less than 0.14 GeV. We require that both pions be positively identified with 85–98% efficiency for real pions, and a misidentification rate of < 5% for low-momentum electrons and < 1% for kaons and protons. The pion candidates are required to form a vertex with $\chi^2_{\text{vtx}} < 20$ (1 degree of freedom) displaced in the transverse plane by at most 2 mm from the e^+e^- interaction region. The transverse momentum of the pion pair is required to satisfy $p_{T\pi\pi} < 0.5$ GeV, and we reject events if any track has $p^* > 1$ GeV.

We further reduce the background by combining several kinematic variables of the dipion system [7] into a multilayer perceptron neural network discriminant (NN) [20]. The NN is trained with a sample of simulated signal events $\Upsilon(1S) \rightarrow \gamma\chi\bar{\chi}$ ($m_\chi = 0$) and an off-peak sample for background; the NN assigns a value \mathcal{N} close to +1 for signal and close to -1 for background. We require $\mathcal{N} > 0.65$ in the low-mass region. This selection has an efficiency of 87% for signal and rejects 96% of the continuum background. In the high-mass region we require $\mathcal{N} > 0.89$ (73% signal efficiency, 98% continuum rejection).

Two additional requirements are applied to reduce specific background contributions. Neutral hadrons from the radiative decays $\Upsilon(1S) \rightarrow \gamma K_L^0 K_L^0$ and $\Upsilon(1S) \rightarrow \gamma n\bar{n}$ may not be detected in the EMC. We remove 90% of

$\mathcal{B}(\Upsilon(1S) \rightarrow \gamma pp\bar{p})$ to $\mathcal{B}(\Upsilon(1S) \rightarrow \gamma nn\bar{n})$. A small additional contribution arises from $\Upsilon(1S) \rightarrow \gamma\pi^+\pi^-$ events in which the pions escape detection. We expect $N_{\text{hadr}} = 6.6 \pm 1.1$ radiative hadronic events (without IFR veto), dominated by $\Upsilon(1S) \rightarrow \gamma K_L^0 K_L^0$, or $N_{\text{hadr}}^{\text{veto}} = 1.02 \pm 0.14$ events (with IFR veto). We describe the M_X^2 distribution of these events with a combination of CB functions, using the measured spectrum of $\Upsilon(1S) \rightarrow \gamma h^+h^-$ events [21].

The largest systematic uncertainty is on the reconstruction efficiency, which includes the trigger/filter efficiency ($\varepsilon_{\text{trig}}$), and photon (ε_γ) and dipion ($\varepsilon_{\pi\pi}$) reconstruction and selection efficiencies. We measure the product $\varepsilon_{\pi\pi} \times N_{\Upsilon(1S)}$, where $N_{\Upsilon(1S)}$ is the number of produced $\Upsilon(1S)$ mesons, with a clean high-statistics sample of the $\Upsilon(1S) \rightarrow \mu^+\mu^-$ decays. The uncertainty (2.1%) is dominated by $\mathcal{B}(\Upsilon(1S) \rightarrow \mu^+\mu^-)$ (2%) [3] and a small selection uncertainty for the $\mu^+\mu^-$ final state. We measure ε_γ in an $e^+e^- \rightarrow \gamma\gamma$ sample in which one of the photons converts into an e^+e^- pair in the detector material (1.8% uncertainty). The trigger efficiency $\varepsilon_{\text{trig}}$ is measured in unbiased random samples of events that bypass the trigger/filter selection. This uncertainty is small for the single-photon triggers (0.4%), but is statistically limited for the dipion triggers (8%). In the low-mass region, we take into account the anti-correlation between single-photon and dipion trigger efficiencies in L3; the uncertainty for the combination of the triggers is 1.2%.

We account for additional uncertainties associated with the signal and background PDFs, and the predicted number of radiative hadronic events N_{hadr} , including PDF parameter correlations. These uncertainties do not scale with the signal yield, but are found to be small. We also test for possible biases in the fitted value of the signal yield with a large ensemble of pseudo-experiments. The biases are consistent with zero for all values of m_{A^0} and m_χ , and we assign an uncertainty of 0.25 events.

As a first step in the likelihood scan, we perform fits to the low-mass and high-mass regions with $N_{\text{sig}} = 0$. The free parameters in the fit are N_{cont} , N_{lept} , and N_{hadr} (low-mass region), and N_{cont} , N_{lept} , and $N_{\eta'}$ (high-mass region). The results of the fits are shown in Fig. 1. We observe no significant deviations from the background-only hypothesis. We find $N_{\text{hadr}} = 8.7^{+4.0}_{-3.3} \pm 0.8$ (without IFR veto) with a significance of 3.5σ , including systematic uncertainties.

We then proceed to perform the likelihood scans as a function of N_{sig} in steps of m_{A^0} and m_χ . In the scan, the contribution of radiative hadronic background is fixed to the expectation $N_{\text{hadr}} = 1.02 \pm 0.14$ for $m_{A^0} < 4$ GeV ($m_\chi < 2$ GeV) where the IFR veto is applied, and to $N_{\text{hadr}} = 6.6 \pm 1.1$ for fits in $4 \leq m_{A^0} \leq 8$ GeV ($2 \leq m_\chi < 4$ GeV) range. We do not observe a significant excess of events above the background, and set upper limits on $\mathcal{B}(\Upsilon(1S) \rightarrow \gamma A^0) \times \mathcal{B}(A^0 \rightarrow \text{invisible})$ (Fig. 2) and $\mathcal{B}(\Upsilon(1S) \rightarrow \gamma\chi\bar{\chi})$ (Fig. 3). The limits are dominated by statistical uncertainties. The largest statistical fluctua-

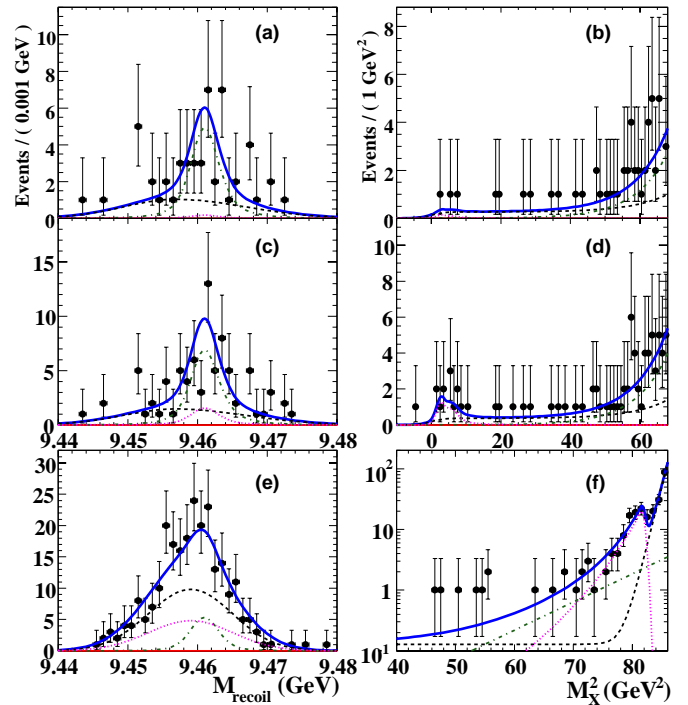


FIG. 1: Projection plots from the fit with $N_{\text{sig}} = 0$ onto (a,c,e) M_{recoil} and (b,d,f) M_X^2 . (a,b): low-mass region with IFR veto; (c,d): low-mass region without IFR veto; (e,f): high-mass region. Overlaid is the fit with $N_{\text{sig}} = 0$ (solid blue line), continuum background (black dashed line), radiative leptonic $\Upsilon(1S)$ decays (green dash-dotted line), and (c,d) radiative hadronic $\Upsilon(1S)$ decays or (e,f) η' background (magenta dotted line).

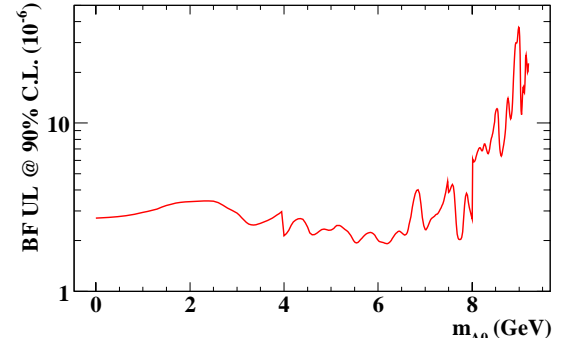


FIG. 2: 90% C.L. upper limits for $\mathcal{B}(\Upsilon(1S) \rightarrow \gamma A^0) \times \mathcal{B}(A^0 \rightarrow \text{invisible})$.

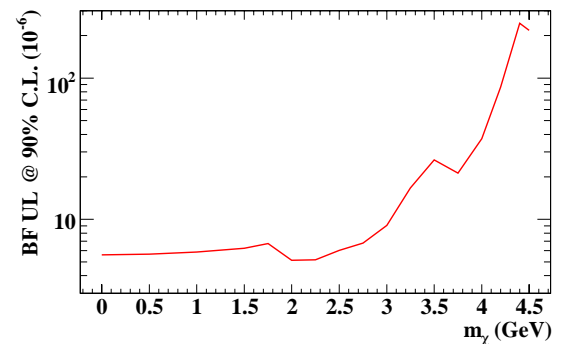


FIG. 3: 90% C.L. upper limits for $\mathcal{B}(\Upsilon(1S) \rightarrow \gamma\chi\bar{\chi})$.

tion, 2.0σ , is observed at $m_{A^0} = 7.58$ GeV [26]; we estimate the probability to see such a fluctuation *anywhere* in our dataset to be over 30%.

In summary, we find no evidence for the single-photon decays $\Upsilon(1S) \rightarrow \gamma + \text{invisible}$, and set 90% C.L. upper limits on $\mathcal{B}(\Upsilon(1S) \rightarrow \gamma A^0) \times \mathcal{B}(A^0 \rightarrow \text{invisible})$ in the range $(1.9\text{--}4.5) \times 10^{-6}$ for $0 \leq m_{A^0} \leq 8.0$ GeV, $(2.7\text{--}37) \times 10^{-6}$ for $8 \leq m_{A^0} \leq 9.2$ GeV, and scalar A^0 . We limit $\mathcal{B}(\Upsilon(1S) \rightarrow \gamma \chi \bar{\chi})$ in the range $(0.5\text{--}24) \times 10^{-5}$ at 90% C.L. for $0 \leq m_\chi \leq 4.5$ GeV, assuming the phase-space distribution of photons in this final state. Our results improve the existing limits by an order of magnitude or more, and significantly constrain [26] light Higgs boson [13] and light dark matter [8] models.

We are grateful for the excellent luminosity and machine conditions provided by our PEP-II colleagues, and for the substantial dedicated effort from the computing organizations that support *BABAR*. The collaborating institutions wish to thank SLAC for its support and kind hospitality. This work is supported by DOE and NSF (USA), NSERC (Canada), CEA and CNRS-IN2P3 (France), BMBF and DFG (Germany), INFN (Italy), FOM (The Netherlands), NFR (Norway), MES (Russia), MICIIN (Spain), STFC (United Kingdom). Individuals have received support from the Marie Curie EIF (European Union), the A. P. Sloan Foundation (USA) and the Binational Science Foundation (USA-Israel).

-
- [2] G. Bertone, D. Hooper, and J. Silk, Phys. Rep. **405**, 279 (2005).
 - [3] K. Nakamura *et al.*, (Particle Data Group), Journal of Physics G **37**, 075021 (2010).
 - [4] J. F. Gunion, D. Hooper, and B. McElrath, Phys. Rev. D **73**, 015011 (2006).
 - [5] P. Jean *et al.*, Astron. Astrophys. **407**, L55 (2003); J. Knodlseder *et al.*, Astron. Astrophys. **411**, L457 (2003).
 - [6] R. Bernabei *et al.* (DAMA Collaboration), Eur. Phys. J. C**56**, 333 (2008).
 - [7] B. Aubert *et al.* (*BABAR* Collaboration), Phys. Rev. Lett. **103**, 251801 (2009).
 - [8] G. Yeghiyan, Phys. Rev. D **80**, 115019 (2009).
 - [9] R. McElrath, preprint arXiv:0712.0016 [hep-ph] (2007); P. Fayet, Phys. Rev. D **81**, 054025 (2010).
 - [10] F. Wilczek, Phys. Rev. Lett. **39**, 1304 (1977).
 - [11] R. Dermisek and J. F. Gunion, Phys. Rev. Lett. **95**, 041801 (2005).
 - [12] M. Lisanti and J. G. Wacker, Phys. Rev. D **79**, 115006 (2009).
 - [13] R. Dermisek, J. F. Gunion, and B. McElrath, Phys. Rev. D **76**, 051105 (2007); R. Dermisek and J. F. Gunion, Phys. Rev. D **81**, 075003 (2010).
 - [14] R. E. Shrock and M. Suzuki, Phys. Lett. **B110**, 250 (1982).
 - [15] R. Balest *et al.* (*CLEO* Collaboration), Phys. Rev. D **51**, 2053 (1995).
 - [16] E. Fullana and M. A. Sanchis-Lozano, Phys. Lett. B **653**, 67 (2007).
 - [17] B. Aubert *et al.* (*BABAR* Collaboration), Nucl. Instrum. Methods Phys. Res., Sect. A **479**, 1 (2002).
 - [18] W. Menges, IEEE Nucl. Sci. Symp. Conf. Rec. **5**, 1470 (2006).
 - [19] Henceforth, * marks CM quantities.
 - [20] A. Höcker *et al.*, preprint physics/0703039, PoS ACAT, 040 (2007); <http://tmva.sourceforge.net/>.
 - [21] S. B. Athar *et al.* (*CLEO* Collaboration), Phys. Rev. D **73**, 032001 (2006).
 - [22] G. Punzi, preprint physics/0308063 (2003).
 - [23] S. Agostinelli *et al.* (*GEANT4* Collaboration), Nucl. Instrum. Methods Phys. Res., Sect. A **506**, 250 (2003).
 - [24] D. Lange, Nucl. Instrum. Methods Phys. Res., Sect. A **462**, 152 (2001).
 - [25] M. J. Oreglia, Ph.D Thesis, report SLAC-236 (1980), Appendix D.
 - [26] Additional plots are available in the Appendix.

* Now at Temple University, Philadelphia, Pennsylvania 19122, USA

[†] Also with Università di Perugia, Dipartimento di Fisica, Perugia, Italy

[‡] Also with Università di Roma La Sapienza, I-00185 Roma, Italy

[§] Now at University of South Alabama, Mobile, Alabama 36688, USA

[¶] Also with Università di Sassari, Sassari, Italy

[1] E. Komatsu *et al.* (WMAP Collaboration), Astrophys. J. Suppl. **180**, 330 (2009); M. Tegmark *et al.* (SDSS Collaboration), Phys. Rev. D **74**, 123507 (2006).

APPENDIX: EPAPS MATERIAL

The following includes supplementary material for the Electronic Physics Auxiliary Publication Service.

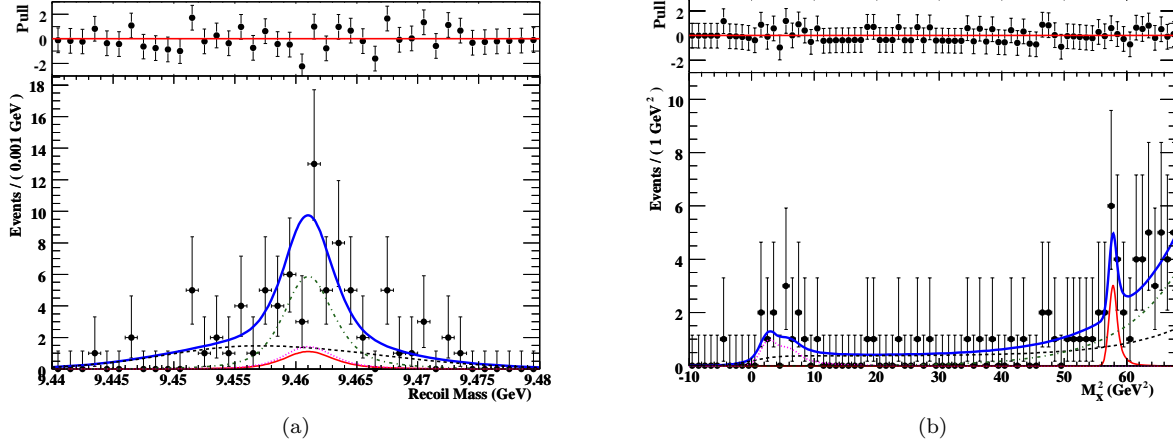


FIG. 4: Projection plots from the fit with $m_{A^0} = 7.58 \text{ GeV}$ (the most significant deviation from zero) to (a) M_{recoil} and (b) M_X^2 . Overlaid is the fit (solid blue line), signal contribution (solid red line), continuum background (black dashed line), radiative leptonic $\Upsilon(1S)$ decays (green dash-dotted line), and radiative hadronic $\Upsilon(1S)$ decays (magenta dotted line). The top plot show residuals in each bin, normalized by the bin error. The fit corresponds to $\mathcal{B}(\Upsilon(1S) \rightarrow \gamma A^0) \times \mathcal{B}(A^0 \rightarrow \text{invisible}) = (3.2^{+2.2}_{-1.8} \pm 1.0) \times 10^{-6}$, where the first uncertainty is statistical and the second is systematic, and statistical significance of 2.0σ . The probability to observe such a fluctuation *anywhere* in our dataset is over 30%.

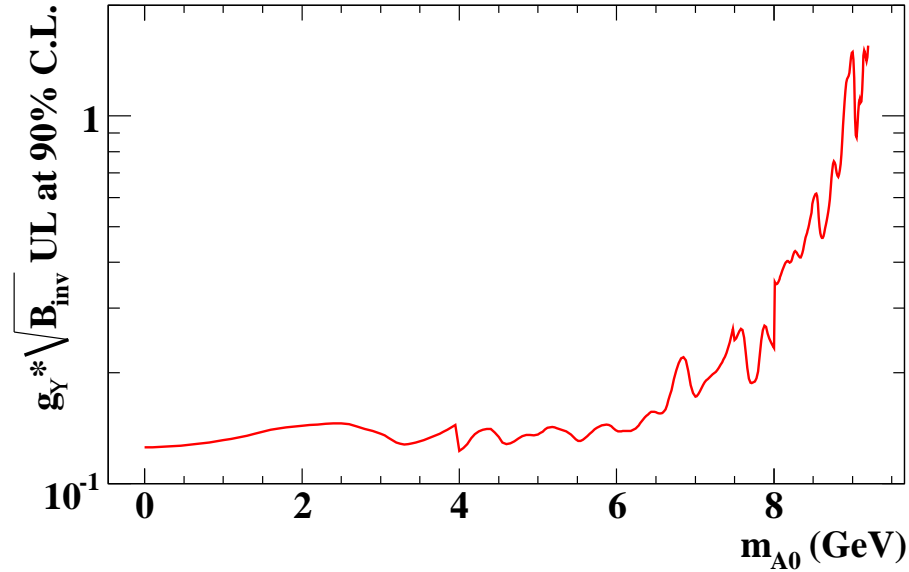


FIG. 5: Upper limits on the product $g_Y \times \sqrt{\mathcal{B}(A^0 \rightarrow \text{invisible})}$ at 90% C.L. as a function of m_{A^0} . The parameter g_Y is an effective coupling of the CP-odd Higgs A^0 to bound state $\Upsilon(1S)$; in NMSSM, $g_Y = \tan \beta \cos \theta F_Y$, where $\cos \theta$ is the fraction of non-singlet component in A^0 , $\tan \beta$ is the ratio of Higgs vacuum expectation values, and F_Y is the effective form-factor (including the QCD and QED corrections). The theoretically preferred region in NMSSM [13] is $g_Y > 1$.